2020 IEEE International Conference on Robotics and Automation (ICRA)
31 May - 31 August, 2020. Paris, France

Geometric Characterization of Two-Finger Basket Grasps of 2-D Objects: Contact Space Formulation

Elon D. Rimon† and Florian T. Pokorny‡ and Weiwei Wan∀

Abstract *This paper considers* basket grasps, *where a two-finger robot hand forms a basket that can safely lift and carry rigid objects in a 2-D gravitational environment. The two-finger basket grasps form special points in a high-dimensional configuration space of the object and two-finger robot hand. This paper establishes that all two-finger basket grasps can be found in a low-dimensional* contact space *that parametrizes the two-finger contacts along the supported object boundary. Using contact space, each basket grasp is associated with its depth that provides a security measure while carrying the object, as well as its safety margin away from a critical finger opening where the object drops-off into its intended destination. Geometric techniques that compute the depth and drop-off finger opening are described and illustrated with detailed graphical and numerical examples.*

I. Introduction

Basket grasps offer a robust approach for picking objects from a clatter, carrying them in a secure manner to their destination, then releasing the objects in a controlled manner by opening the basket formed by the robot hand. Important applications include packing orders at logistic centers and picking up parts that arrive in a clutter during manufacturing operations [5, 6, 8, 9, 11, 12, 21]. This paper establishes that all two-finger basket grasps as well as their depth and drop-off finger opening can be found in a low-dimensional *contact space,* which parametrizes the two-finger contacts along the object boundary.

We study *basket grasps* of polygonal objects in a 2-D gravitational environment. The robot hand is modeled as two point or disc-fingers that freely move in $I\!R^2$. The object, $\mathcal{B}$, is initially supported at an equilibrium stance (Fig. 1(a)). The object is to be lifted and carried in a safe manner by a *basket* formed by a two-finger robot hand, where safety is measured by the *depth* of the basket formed by the supporting fingers. The fingers retain their relative distance and orientation while carrying the object (Fig. 1(b)), and the hand should be able to drop the object in a predictable manner upon reaching the intended destination.

Basket grasps form a special class of *caging grasps* [17, 20]. In *basket grasps,* the bounded mobility of the carried object is based on rigid-body constrains imposed by the supporting fingers and energy-bound imposed on the object motions within the basket. Hence, efficient caging grasp techniques can be leveraged to the synthesis of basket grasps [10, 13, 23]. Mahler et al. [13] were the first to offer an algorithm that computes basket grasps for two-finger robot hands. Their sampling based technique computes a bound on the depth (and hence security) of candidate basket grasps. Among the *caging* techniques surveyed by Makita and Wan [14] and the *Robot Grasping* text [18], let us shed light on two approaches. The first approach was pioneered by Vahedi [22], and arrived to full maturity in the work of Pipattanasomporn [15, 16]. Under this approach, the physical space surrounding the grasped object is partitioned into convex cells. A search graph whose nodes represent the placement of the k robot fingers in these cells is then used to compute all caging grasps surrounding a given object, often as a convex optimization problem per grasp node. These techniques compute all two-finger caging grasps of polygonal objects with n edges in $O(n^2 \log n)$ steps, and all three-finger caging grasps in $O(n^3 \log n)$ steps. However, this approach requires a high-dimensional configuration space for the freely moving finger bodies.

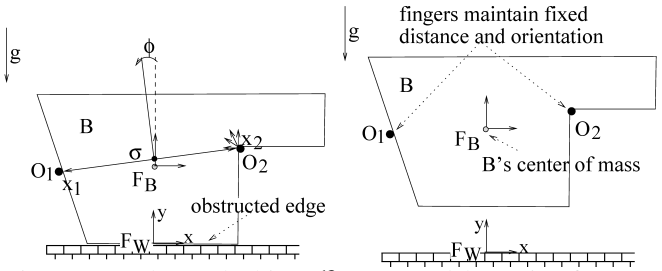

Fig. 1: A polygonal object $\mathcal{B}$ supported by point fingers $\mathcal{O}_1$ and $\mathcal{O}_2$ in a basket grasp (the full robot hand is not shown). The parameter σ describes the inter-finger distance, ϕ measures the two-fingers' orientation relative to gravity.

In his PhD thesis [1], Allen pioneered an alternative approach that uses a low-dimensional *contact space* to compute caging grasps. Under the contact space approach, the fingers maintain contact with the grasped object during the search for caging grasps, thus reducing the search space into a low-dimensional contact space that can be intuitively verified as motion of the fingers along the object boundary. Allen showed that all two-finger caging grasps can be computed in contact space using $O(n^2 \log n)$ steps [2]. Bunis [4] used contact space to compute all three-finger caging grasps that maintain similar triangular formations using $O(n^3 \log n)$ steps. Bunis [3] subsequently used contact space to compute all two-finger *locking grasps* of 2-D objects against a wall using the same number of steps.

Motivated by the contact space approach, this paper describes how the layout and properties of two-finger basket grasps can be computed in the low-dimensional contact space. The *basket grasps* form special points in a five-dimensional *configuration space* (*c-space*) of the object and two-finger hand. This space consists of the grasped

†Dept. of ME, Technion, Israel. ‡Dept. of EECS, KTH Royal Inst. of Technology, Sweden. ∀School of Eng. Science, Osaka University, Japan.

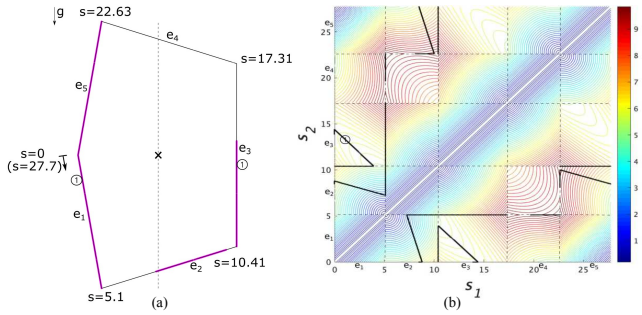

Fig. 2: (a) The s-parameterization of the object boundary. (b) The object's contact space $\mathcal{U}$ for two point fingers, overlayed with the contours of the function $\sigma(s_1, s_2)$.

object configurations, $q \in I\!R^3$, the finger-opening parameter $\sigma \geq 0$, and the angle ϕ of the two-finger system relative to gravity (Fig. 1(a)). When the object waiting to be lifted is located at a configuration q_0, the high-dimensional configuration space contains a 2-D submanifold of all two-finger contacts along the object boundary positioned at q_0. This submanifold is parametrized in terms of *contact space,* which is then used to compute the layout of all possible basket grasps of an object waiting to be lifted.

The paper describes a geometric technique that determines the *depth* (and hence security) of a candidate basket grasp. The main result of the paper, the *basket grasp theorem,* states that the depth of a basket grasp is determined by the relative height of the object's center of mass at specific single- and two-finger equilibrium stances associated with the basket grasp. These stances can be readily found and sorted in contact space as demonstrated with detailed examples. The paper finally addresses the *drop-off problem,* where the fingers open along a fixed line in $I\!R^2$ until a critical drop-off event is reached. This critical finger opening is associated with a frictionless two-finger equilibrium grasp of the object (without gravity), that can be efficiently computed by a simple contact space search.

Section II introduces the notion of *contact space* and characterizes the layout of all possible two-finger basket grasps at a given object position using contact space. Section III describes a geometric technique that uses contact space to determine the *depth* of a candidate basket grasp. Section IV demonstrates the technique on several object types. Section V studies the *drop-off problem,* where contact space is used to search for the critical drop-off finger opening of a given basket grasp. The conclusion discusses open problems as well as extension to 3-D basket grasps.

II. Contact Space of Two-Finger Basket Grasps

This section characterizes the two-finger basket grasps of a 2-D object at a given initial position using *contact space.* The object's outer boundary is parametrized by arclength in counterclockwise direction using the parameter $s \in [0, L]$, where L is the object's perimeter (Fig. 2(a)). Let $p(s_1)$ and $p(s_2)$ denote the position of the finger contacts along the object boundary, such that $p_1(0)=p_1(L)$ and $p_2(0)=p_2(L)$.

Definition 1. *A polygonal object $\mathcal{B}$ is contacted by two fingers at $p(s_1)$ and $p(s_2)$. **Contact space** is the parameterization of all two-finger contacts along the object boundary, given by the set $\mathcal{U} = [0, L] \times [0, L]$ in the (s_1, s_2) plane.*

Contact space consists of *rectangles,* each associated with a particular pair of object edges (including same-edge pairs). The lines bounding each rectangle represent vertex-edge contacts. The *diagonal,* $\Delta = \{(s_1, s_2) \in \mathcal{U} : s_1 = s_2\}$, represents all two-finger pinchings along the object boundary. The diagonal forms an *obstacle* in $\mathcal{U}$, since the fingers may not cross each other while moving along the object boundary.

Example: Consider the inter-finger distance function defined in $\mathcal{U}$ as $\sigma(s_1, s_2) = \|p(s_1) - p(s_2)\|$. The contours of $\sigma(s_1, s_2)$ in $\mathcal{U}$ are depicted Figure 2(b). Note that $\sigma(s_1, s_2)$ is non-negative and continuous on $\mathcal{U}$, and attains a global minimum of zero along the diagonal Δ. Also note that $\sigma(s_1, s_2)$ forms a positive definite quadratic function in the individual contact space rectangles. ◦

When a rigid object $\mathcal{B}$ is supported by finger bodies $\mathcal{O}_1$ and $\mathcal{O}_2$ at an *equilibrium stance,* the net wrench on $\mathcal{B}$ due to gravity and the supporting contacts must be zero. The next lemma characterizes the two-finger equilibrium stances in contact space $\mathcal{U}$ (see [19]).

Lemma II.1. *Let a polygonal object $\mathcal{B}$ be located at a configuration q_0 in a 2-D gravitational environment. All two-finger contacts that form feasible equilibrium stances generically form* **piecewise linear curves** *in $\mathcal{U}$.*

Example: Fig. 2(a) shows a polygonal object $\mathcal{B}$ at a fixed position-and-orientation in $I\!R^2$. Fig. 2(b) shows in solid black all two-finger placements along the object boundary that form feasible equilibrium stances in contact space $\mathcal{U}$. ◦

To describe the object's gravitational potential energy, let b_{cm} denote the position of $\mathcal{B}$'s center of mass in $\mathcal{B}$'s reference frame $\mathcal{F}_B$ ($b_{cm} = \vec{0}$ in Fig. 1). When $\mathcal{B}$ is located at a configuration $q = (d, \theta)$, the position of its center of mass in the fixed world frame, $\mathcal{F}_W$, is given by $X_{cm}(q) = R(\theta)b_{cm} + d$, where $q = (d, \theta) \in I\!R^3$. The *gravitational potential energy* of $\mathcal{B}$ is given by $U(q) = mg\big(\boldsymbol{e} \cdot X_{cm}(q)\big)$, where m is $\mathcal{B}$'s mass, g is the gravitational constant, and $\boldsymbol{e}$ is the vertical upward direction, $\boldsymbol{e} = (0, 1)$, in $I\!R^2$. The function $U(q)$ simply measures the height of $\mathcal{B}$'s center of mass in $\mathcal{F}_W$. The gravitational wrench affecting $\mathcal{B}$ is given by $-\nabla U(q) = -mg(\boldsymbol{e}, R(\theta)b_{cm} \times \boldsymbol{e})$ (see [19]).

Consider the free c-space, $\mathcal{F}$, whose c-obstacles are induced by fixed supporting fingers $\mathcal{O}_1$ and $\mathcal{O}_2$. Based on conservation of energy, the non-degenerate local minima of $U(q)$ in $\mathcal{F}$ form *locally stable* equilibrium stances of the object $\mathcal{B}$. This property is the basis for the following definition of *basket grasps.*

Definition 2. *Let a rigid object $\mathcal{B}$ be supported under gravity by fingers $\mathcal{O}_1$ and $\mathcal{O}_2$ at an equilibrium stance configuration q_0. The supporting fingers form a* **basket grasp** *if q_0 forms a non-degenerate local minimum of $U(q)$ in $\mathcal{F}$.*

The local-minimum test of $U(q)$ in contact space $\mathcal{U}$ depends on the height of $\mathcal{B}$'s center of mass as follows [19].

Lemma II.2. *A two-finger equilibrium stance that involves two edges of $\mathcal{B}$ forms a* **local minimum** *of $U(q)$ when $-\lambda_1(\rho_1(s_1, s_2) + r_{\mathcal{O}_1}) - \lambda_2(\rho_2(s_1, s_2) + r_{\mathcal{O}_2}) + y_{\mathsf{cm}}(s_1, s_2) < 0$ where $\lambda_1, \lambda_2 \geq 0$ are the equilibrium stance coefficients,*

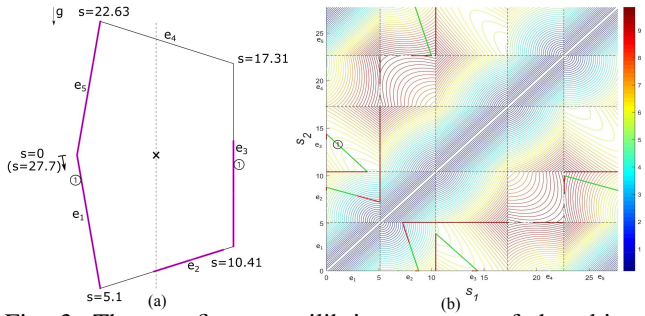

Fig. 3: The two-finger equilibrium stances of the object shown in Figure 2 are either local-minima (green) or local-maxima (red) of $U(q)$ in contact space (see text).

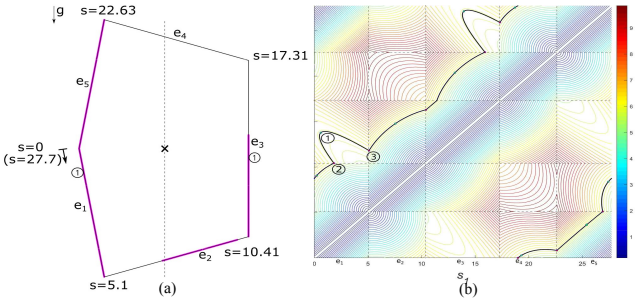

Fig. 4: (a) A polygonal object supported at a two-finger basket grasp. (b) The σ_0-contour of $\sigma(s_1, s_2)$ in $\mathcal{U}$.

ρ_1, ρ_2 are the signed distances of the contacts from the intersection point, p, of the finger contact normals, $r_{\mathcal{O}_1}, r_{\mathcal{O}_2} \geq 0$ the finger radii, and y_{cm} the height of $\mathcal{B}$'s center of mass above p. Stances that involve a concave vertex and an edge of $\mathcal{B}$ generically form **local minima** *of $U(q)$.*[1]

Example: The equilibrium stances of Figure 2 are color-coded according to their stability type in Figure 3. Green for the local minima and red for the local maxima of $U(q)$ in $\mathcal{U}$. The stability type of each stance describes how the height of $\mathcal{B}$'s center of mass changes when the object moves in contact with two fixed point or disc fingers. ◦

Remark: A two-finger *basket grasp* of $\mathcal{B}$ is a non-degenerate local minimum of $U(q)$ in the free c-space, $\mathcal{F}$, whose finger c-obstacles are $\mathcal{CO}_1$ and $\mathcal{CO}_2$. A basket grasp of $\mathcal{B}$ is an equilibrium stance that forms a *local minimum* of $U(q)$ along the 1-D stratum $\mathcal{S} = \mathsf{bdy}(\mathcal{CO}_1) \cap \mathsf{bdy}(\mathcal{CO}_2)$ in $\mathcal{F}$. The stratum $\mathcal{S}$ corresponds to the contour of $\sigma(s_1, s_2)$ that passes through the basket-grasp point in $\mathcal{U}$. Hence, when the *puncture point* that determines the depth of the basket grasp occurs at a two-finger stance, it forms a *local maximum* of $U(q)$ along the basket-grasp contour in $\mathcal{U}$. ◦

III. Contact Space Computation of Basket-Grasp Depth

This section describes a technique that determines the *depth* (and hence security) of a candidate basket grasp. The technique is described for *point fingers* then extended to disc fingers. In a basket grasp, the object's configuration point, q_0, lies at the bottom a 3-D cavity in the free c-space $\mathcal{F}$ [19]. As the level-set of $U(q)$ increases its height in $\mathcal{F}$, the appearance of a *puncture point,* q_1, marks the *depth* of the basket grasp. The basket grasp is specified as two finger contacts on the object boundary, $(s_1^0, s_2^0) \in \mathcal{U}$, at the object configuration q_0. The fingers now become *fixed supports* with fixed inter-finger distance, $\sigma_0 = \|p(s_1^0) - p(s_2^0)\|$.

The technique computes the basket grasp depth by tracing the σ_0-contour of $\sigma(s_1, s_2)$ in $\mathcal{U}$, which represents object motions that maintain contact with the supporting fingers. The following lemma characterizes the σ_0-contour.

Lemma III.1 ([2])**.** *Each contour of $\sigma(s_1, s_2)$ in $\mathcal{U}$ consists of* **elliptical and linear segments** *associated with the contact-space rectangles, with vertices on the rectangles' bounding lines* (Figure 4(b)).

The elliptical contour segments can be parametrized in terms of $\mathcal{B}$'s orientation, θ, in each rectangle $\mathcal{R}_{jk}$ as follows. Let t_j and t_k denote the unit tangents to the edges e_j and e_k of $\mathcal{B}$. Then each contour segment is given by

$$\begin{pmatrix} s_1(\theta) \\ s_2(\theta) \end{pmatrix} = A^{-1}\big(R^T(\theta)(x_1 - x_2) + p_k^0 - p_j^0\big) \quad \theta \in [\theta_{jk}^-, \theta_{jk}^+] \tag{1}$$

where $A = [t_j \; -t_k]$, p_j^0, p_k^0 are the initial vertices of e_j and e_k, and x_1, x_2 are the point-finger positions. The endpoint angles θ_{jk}^- and θ_{jk}^+ occur when one of the two fingers touches an endpoint of the respective object edge. When the two fingers support the same edge (or parallel edges) of $\mathcal{B}$, the object maintains fixed orientation θ along a linear contour segment. The segment satisfies the constraint $s_2 + s_1 = c$, where $c = t_j \cdot (R^T(\theta)(x_1 - x_2) + p_k^0 - p_j^0)$ is constant.

Example: Figure 4(a) shows a polygonal object $\mathcal{B}$ supported by two fingers at a local minimum (i.e. a basket grasp) of $U(q)$. The fingers remain fixed in $I\!R^2$ while $\mathcal{B}$ moves along the σ_0-contour depicted in Figure 4(b). ◦

Starting at the basket-grasp point, $v_0 = (s_1^0, s_2^0)$, the technique traces the σ_0-contour in stages that correspond to the contact-space rectangles and their bounding lines. The contour is searched sequentially along its two directions. The θ-parametrization of Eq. (1) can be used to compute the endpoints of the initial contour segments that start at v_0 and reach the contact-space rectangle bounding lines, at v_1^- and v_1^+. In all subsequent stages, the technique constructs the contour segments that start at the points v_i^- and v_i^+ and end at the points v_{i+1}^- and v_{i+1}^+ located on the next contact-space rectangles bounding lines. This process ends when the first two-finger equilibrium stance is encountered along each direction, as next described.

Edge-edge equilibrium stance: Consider a stance that involves two edges e_j and e_k of $\mathcal{B}$, with inward unit normals n_j and n_k. The force-part of the equilibrium stance condition requires that $\lambda_1 R(\theta) n_j + \lambda_2 R(\theta) n_k = \boldsymbol{e}$ for some $\lambda_1, \lambda_2 \geq 0$. As described in [19], $\lambda_1, \lambda_2 \geq 0$ form inequality constraints in θ that determine a θ-interval denoted $\mathcal{I}_{jk}$. The moment-part of the equilibrium stance forms the constraint:

$$\det \begin{bmatrix} R(\theta) n_j & R(\theta) n_k & \boldsymbol{e} \\ p(s_1(\theta)) \times n_j & p(s_2(\theta)) \times n_k & 0 \end{bmatrix} = 0 \quad \theta \in \mathcal{I}_{jk}.$$

The solutions of this equation in θ give the edge-edge equilibrium stances along the σ_0-contour in the rectangle $\mathcal{R}_{jk}$.

[1] Stances that involve disc-fingers located at convex vertices of $\mathcal{B}$ typically do not form local-minima of $U(q)$ (see [19]).

Vertex-edge equilibrium stance: Let the fingers support the j'th vertex of $\mathcal{B}$ at $p(s_1)$, and the edge e_k of $\mathcal{B}$ at $p(s_2)$. The object orientation, θ, is fixed at this particular (s_1, s_2) point. To check equilibrium stance feasibility, one models the finger at the vertex as a disc of small radius $\epsilon > 0$. Let e_{j1} and e_{j2} be the two edges of $\mathcal{B}$ that meet at the vertex, with inward unit normals n_{j1} and n_{j2}. The disc-finger can realize any contact force direction within the *generalized contact normal* at the vertex, $\lambda_{11} n_{j1} + \lambda_{12} n_{j2}$ such that $\lambda_{11}, \lambda_{12} \geq 0$. The equilibrium stance force-part requires that $\lambda_{11} R(\theta) n_{j1} + \lambda_{12} R(\theta) n_{j2} + \lambda_2 R(\theta) n_k = \boldsymbol{e}$ for some $\lambda_{11}, \lambda_{12}, \lambda_2 \geq 0$. The solution determines a sector of force directions at the object vertex, $\lambda n_{j1} + (1-\lambda) n_{j2}$, such that λ varies in an interval $\mathcal{I}_j$ contained in $[0, 1]$. The moment-part of the equilibrium stance forms the constraint:

$$\det \begin{bmatrix} \lambda \bar{n}_{j1} + (1-\lambda)\bar{n}_{j2} & R(\theta) n_k & \boldsymbol{e} \\ p(s_1(\theta)) \times (\lambda \bar{n}_{j1} + (1-\lambda)\bar{n}_{j2}) & p(s_2(\theta)) \times n_k & 0 \end{bmatrix} = 0$$

where $\bar{n}_{j1} = R(\theta) n_{j1}$ and $\bar{n}_{j2} = R(\theta) n_{j2}$. A solution $\lambda \in \mathcal{I}_j$ identifies the feasibility of a vertex-edge equilibrium stance at an endpoint of the σ_0-contour segment in $\mathcal{R}_{jk}$.

Example: The σ_0-contour depicted in Figure 4(b) contains the basket-grasp point (green dot no. 1). The neighboring *local maxima* of $U(q)$ along the σ_0-contour form vertex-edge equilibrium stances (red dots no. 2 and 3). ∘

The technique compares the heights of $\mathcal{B}$'s center of mass at the two-finger equilibrium stances located on the σ_0-contour, taking into account the relevant single-finger equilibrium stances as summarized in the following theorem.

Theorem 1 (Basket Depth). *Let two finger contacts at (s_1^0, s_2^0) form a basket grasp of a 2-D object $\mathcal{B}$ at q_0. Let (s_1^-, s_2^-) and (s_1^+, s_2^+) be the two-finger equilibrium stances encountered along both directions of the basket-grasp contour in $\mathcal{U}$. Let h^- and h^+ be the height of $\mathcal{B}$'s center of mass at these stances. Let h_i be the minimum height of $\mathcal{B}$'s center of mass over the single-finger equilibrium stances along the boundary segment $[s_i^-, s_i^+]$ for $i = 1, 2$. The* **basket-grasp depth** *is given by $\min\{h^-, h^+, h_1, h_2\}$, measured relative to the height of $\mathcal{B}$'s center of mass at q_0.*

Remark: One only needs to check single-finger stances that form *saddle points* of $U(q)$ in $\mathcal{F}$. These are single-finger stances that involve a horizontal edge of $\mathcal{B}$, and certain single-finger stances that involve a vertex of $\mathcal{B}$ (see [19]). ∘

Proof sketch: The 3-D cavity of a basket grasp at q_0 is surrounded by the finger c-obstacles $\mathcal{CO}_1$ and $\mathcal{CO}_2$ and the level-set of $U(q)$ that passes through the *puncture point,* q_1. The puncture point q_1 can appear on the individual c-obstacle boundaries, $\mathcal{S}_1 = \mathsf{bdy}(\mathcal{CO}_1)$ and $\mathcal{S}_2 = \mathsf{bdy}(\mathcal{CO}_2)$, or on their intersection curve $\mathcal{S} = \mathsf{bdy}(\mathcal{CO}_1) \cap \mathsf{bdy}(\mathcal{CO}_2)$. The curve $\mathcal{S}$ corresponds to the σ_0-contour in $\mathcal{U}$ that passes through (s_1^0, s_2^0). Hence, h^- and h^+ measure the height of $\mathcal{B}$'s center of mass at the first local-maxima of $U(q)$ encountered along $\mathcal{S}$, which form *saddle points* of $U(q)$ in $\mathcal{F}$.

If the lowest saddle point of $U(q)$ lies on $\mathcal{S}_i = \mathsf{bdy}(\mathcal{CO}_i)$, consider the *rim curve* defined as the intersection curve $\mathcal{S}_i \cap \{q : U(q) = U(q_1)\}$. It forms a closed loop with constant height in $\mathcal{F}$ that passes through q_1. Since q_1 is the *lowest* saddle point of $U(q)$ just above q_0, the rim curve intersects the 1-D stratum $\mathcal{S}$ at points *lower* than the local-maxima encountered along $\mathcal{S}$. Hence, starting at q_1, the object $\mathcal{B}$ can move along the rim curve while maintaining contact with the single finger $\mathcal{O}_i$, until the other finger is encountered at some point of $\mathcal{S}$. At this instant the object is located at a point (s_1^*, s_2^*) on the σ_0-contour in $\mathcal{U}$. Moreover, (s_1^*, s_2^*) lies on the piece of the σ_0-contour that contains the basket-grasp point (s_1^0, s_2^0) and bounded by the *higher* endpoints (s_1^-, s_2^-) and (s_1^+, s_2^+).

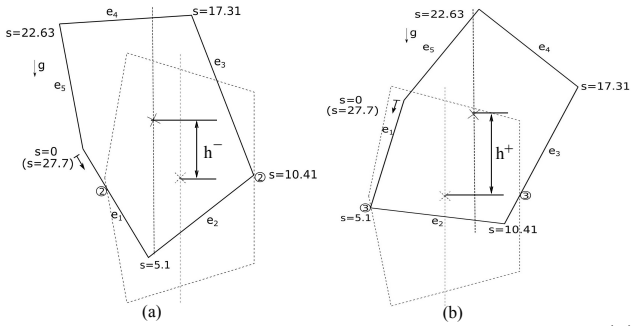

Fig. 5: (a) A two finger vertex-edge saddle point of $U(q)$ with relative height h^-. (b) A two finger vertex-edge saddle point of $U(q)$ with relative height h^+.

When $\mathcal{B}$ moves along the rim-curve segment that starts at q_1, its contact point with $\mathcal{O}_i$ moves in a continuous manner along $\mathcal{B}$'s boundary, until the other finger is encountered at (s_1^*, s_2^*). If the contact point started *outside* $\mathcal{B}$'s boundary segment parametrized by $[s_i^-, s_i^+]$, it must have passed through one of the interval's endpoints, s_i^- or s_i^+, before reaching the point s_i^* that lies *inside* the interval. Since $\mathcal{B}$ maintained a single contact with $\mathcal{O}_i$ during this motion, the contact point at q_1 must be located *inside* $\mathcal{B}$'s boundary segment parametrized by $[s_i^-, s_i^+]$. The heights h_1 and h_2 thus capture all single-finger equilibrium stances that can possibly form the puncture point of the basket grasp. □

Extension to disc fingers: The disc fingers can be converted into point fingers by expanding the boundary of $\mathcal{B}$ outward by the disc-fingers' radius. The boundary of the resulting c-space object, $\mathcal{CB}$, contains straight line edges as well as circular arcs. Every circular arc can be approximated by a regular k-segment polygonal arc. The basket-grasp depth can now be computed on the polygonal approximation of $\mathcal{CB}$. The output will closely approximate the exact basket-grasp depth, and will usually identify the exact object features that determine the basket grasp depth.

IV. Representative Examples

This section illustrates the technique of the previous section on three examples.

Example 1: Consider the basket grasp of the convex object $\mathcal{B}$ depicted earlier in Figure 4 (green dot no. 1). The two *local maxima* of $U(q)$ along the σ_0-contour of the basket grasp form vertex-edge equilibrium stances (red dots no. 2 and 3). These stances are shown in Figure 5 with their relative heights h^- and h^+. The object also possesses two single-finger equilibrium stances along the red boundary segments (see Theorem 1). These stances are shown in Figure 6 with their relative heights h_1 and h_2.

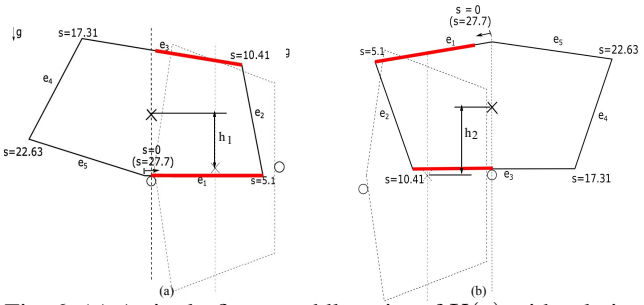

Fig. 6: (a) A single-finger saddle point of $U(q)$ with relative height h_1. (b) A single-finger saddle point of $U(q)$ with relative height h_2.

In this example, the minimum height and hence the *basket grasp depth* is h^-, depicted in Figure 5(a). ○

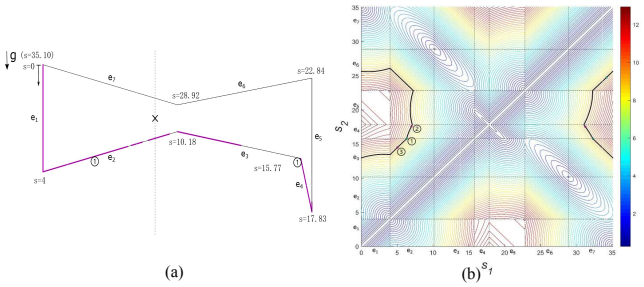

Fig. 7: (a) A non-convex object having a shifted center-of-mass, supported at a two-finger basket grasp. (b) The σ_0-contour of $\sigma(s_1, s_2)$ in $\mathcal{U}$, with the local minimum (no. 1) and two local maxima (no. 2 and 3) of $U(q)$.

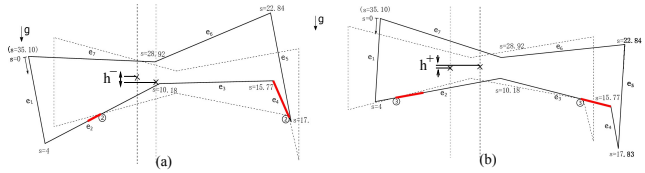

Fig. 8: (a) An edge-edge saddle point of $U(q)$ with relative height h^-. (b) An edge-edge saddle point of $U(q)$ with relative height h^+. The basket grasp depth is h^+.

Example 2: Figure 7(a) shows a non-convex object $\mathcal{B}$ having a shifted center of mass. The object is supported in a basket grasp via an edge and a concave vertex of $\mathcal{B}$. Figure 7(b) shows the basket-grasp point in contact space (green dot no. 1). The two *local maxima* of $U(q)$ along the σ_0-contour of the basket grasp are edge-edge equilibrium stances, located inside the contact-space rectangles (red dots no. 2 and 3). These stances are shown in Figure 8 with their relative heights h^- and h^+. The object has no single-finger equilibrium stances along the red boundary segments (see Theorem 1). The minimum height and hence the *basket grasp depth* is h^+, depicted in Figure 8(b). ○

Example 3: Figure 9(a) depicts a cup-like object supported in a basket grasp via an edge and a concave vertex of $\mathcal{B}$. Figure 9(b) shows the basket-grasp point in contact space (green dot no. 1). The two *local maxima* of $U(q)$ along the σ_0-contour of the basket grasp are located on bounding lines of the respective contact-space rectangles (red dots no. 2 and 3). These stances are shown in Figure 10

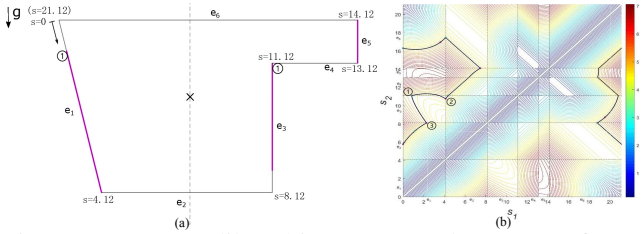

Fig. 9: (a) A cup-like object supported at a two-finger basket grasp. (b) The σ_0-contour of $\sigma(s_1, s_2)$ in $\mathcal{U}$, with the local minimum (no. 1) and two local maxima (no. 2 and 3) of $U(q)$.

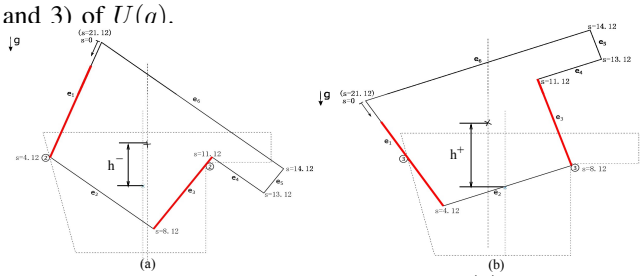

Fig. 10: (a) A vertex-edge saddle point of $U(q)$ with relative height h^-. (b) A vertex-edge saddle point of $U(q)$ with relative height h^+. The basket grasp depth is h^-.

with their relative heights h^- and h^+. There are also two single-finger equilibrium stances along the red boundary segments (see Theorem 1), having higher relative heights h_1 and h_2. The minimum height and hence the *basket grasp depth* is h^-, depicted in Figure 10(a). ○

V. Critical Drop-Off Finger Opening

This section characterizes the critical finger opening of a given basket grasp that allows the release of the object $\mathcal{B}$ at its intended destination. To analyze this problem, we assume that the fingers open along a *fixed line* in $\mathbb{R}^2$, determined by the inter-finger segment at the given basket grasp (Figure 11(a)). The angle between the inter-finger segment and the direction of gravity is thus fixed at $\phi = \phi_0$. Recall that (q_0, σ_0) are the object configuration and inter-finger distance at the initial basket grasp. The *configuration space* of the drop-off problem consists of the coordinates $(q, \sigma) \in \mathbb{R}^4$, where $q \in \mathbb{R}^3$ and $\sigma \geq \sigma_0$.

The (q, σ)-space can be thought of as a one-parameter family of 3-D spaces, $q \in \mathbb{R}^3$, parametrized by σ. For each σ, the fingers form fixed supports while the object moves freely in $\mathbb{R}^2$. Let $\mathcal{CO}_1|_\sigma$ and $\mathcal{CO}_2|_\sigma$ denote the finger c-obstacles in each σ-slice of $\mathbb{R}^4$. The composite finger c-obstacles in $\mathbb{R}^4$ are thus $\cup_{\sigma \geq \sigma_0} \mathcal{CO}_1|_\sigma$ and $\cup_{\sigma \geq \sigma_0} \mathcal{CO}_2|_\sigma$. When the fingers move apart along a fixed line in $\mathbb{R}^2$, the finger c-obstacles move apart as rigid shapes in the corresponding σ-slices of $\mathbb{R}^4$. At $\sigma = \sigma_0$, the finger c-obstacles overlap in a local neighborhood of q_0 (Figure 11(b)). As the fingers move apart, a *drop-off puncture point* will eventually appear between the finger c-obstacles, at a point (q_1, σ_1) such that $\sigma_1 > \sigma_0$ (Figures 11(c)-(d)). The finger opening difference, $\sigma_1 - \sigma_0$, measures the basket grasp's *safety margin* away from the critical drop-off event.

The remainder of this section describes a scheme for computing the drop-off puncture point in contact space $\mathcal{U}$.

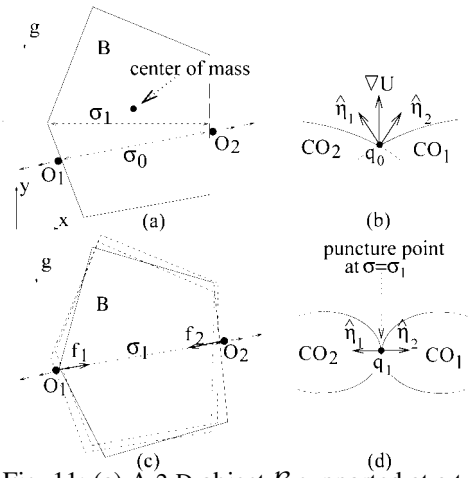

Fig. 11: (a) A 2-D object $\mathcal{B}$ supported at a two-finger basket grasp with inter-finger distance σ_0. (b) Cross section of $(q,\sigma) \in I\!R^4$ at the basket grasp point (q_0, σ_0). (c) The critical drop-off finger opening, σ_1, is a frictionless two-finger equilibrium grasp of $\mathcal{B}$. (d) Cross section of $(q,\sigma) \in I\!R^4$ at the drop-off puncture point (q_1, σ_1).

The σ-slices of (q,σ)-space are level-sets of the scalar valued function $\pi : I\!R^4 \rightarrow I\!R$, defined as $\pi(q,\sigma) = \sigma$. Consider the *free c-space* defined as $I\!R^4 - \mathsf{int}(\mathcal{CO})$, where $\mathcal{CO} = \cup_{\sigma \geq \sigma_0} (\mathcal{CO}_1|_\sigma \cup \mathcal{CO}_2|_\sigma)$ and $\mathsf{int}(\cdot)$ denotes set interior. According to Stratified Morse theory [7], the puncture point (q_1, σ_1) is a *critical point* of $\pi(q,\sigma)$ having the following properties [17]. All critical points of $\pi(q,\sigma)$ in the free c-space occur at *frictionless two-finger equilibrium grasps* of the object $\mathcal{B}$ (without gravity). And all puncture points are *saddle points* of $\pi(q,\sigma)$ in the free c-space.

The set of all two-finger contacts with the object $\mathcal{B}$ forms a 2-D submanifold of $I\!R^4$, parametrized by contact space $\mathcal{U}$. Allen [2] established that the behavior of $\pi(q,\sigma)$ in the free c-space, $I\!R^4$–$\mathsf{int}(\mathcal{CO})$, is in one-to-one correspondence with the behavior of the inter-finger distance function, $\sigma(s_1, s_2)$, in $\mathcal{U}$. In particular, the *saddle points* of $\pi(q,\sigma)$ (which occur at two-finger frictionless equilibrium grasps) appear as *saddle points* of $\sigma(s_1, s_2)$ in $\mathcal{U}$. Hence, the computation of the critical drop-off finger opening reduces to a search for the lowest saddle point of $\sigma(s_1, s_2)$ in $\mathcal{U}$ that retracts under decreasing σ to the basket-grasp point (s_1^0, s_2^0).

The saddle points of $\sigma(s_1, s_2)$ are of two possible types [2]. Equilibrium grasps where one finger contacts a convex vertex while the other finger contacts an opposing edge of $\mathcal{B}$ (Figure 11(c)); or equilibrium grasps that involve a convex vertex and an opposing concave vertex of $\mathcal{B}$. All saddle points are thus located on the *bounding lines* of the contact-space rectangle (at most one on each bounding line segment). Let $\mathcal{R}_{jk}$ be the contact-space rectangle that contains the basket-grasp point (s_1^0, s_2^0). First determine the two endpoints of the σ_0-contour segment of $\sigma(s_1, s_2)$ on bounding linesof $\mathcal{R}_{jk}$. The search can now be thought of as gradually filling contour-segments of $\sigma(s_1, s_2)$ inside $\mathcal{R}_{jk}$ with water, while searching for two-finger equilibrium grasps on the rectangle's bounding lines. As the water rises between successive contour segments according to their σ values, they will eventually reach the lowest saddle point of $\sigma(s_1, s_2)$ that retracts under decreasing σ to the basket-grasp point (s_1^0, s_2^0). This search takes $O(n^2 \log n)$ steps, where n is the number of edges of the object $\mathcal{B}$ [2].

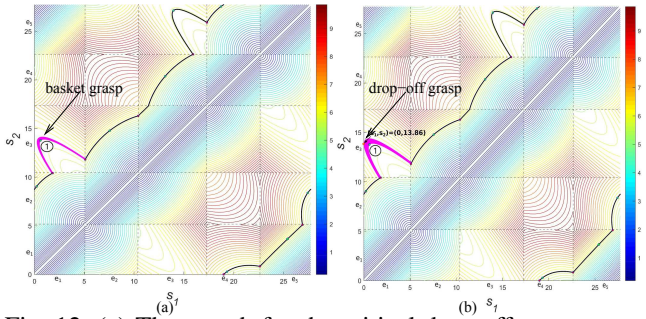

Fig. 12: (a) The search for the critical drop-off event starts with the basket-grasp contour segment. (b) The search ends at the lowest saddle point of $\sigma(s_1, s_2)$, located on the left bounding line of a contact space rectangle $\mathcal{R}_{13}$.

Example: Consider the two-finger basket grasp of the convex object $\mathcal{B}$ depicted earlier in Figure 4 (green dot no. 1). The water filling analogy starts with the σ_0-contour segment of the basket grasp in the rectangle $\mathcal{R}_{13}$ (Figure 12(a)). As the water rises with increasing σ, they reach the frictionless two-finger equilibrium grasp located on the left bounding line of $\mathcal{R}_{13}$. It is a saddle point of $\sigma(s_1, s_2)$ that marks the critical drop-off finger opening of σ_1. ∘

VI. Conclusion

The paper established that the basket grasps can be analyzed and computed in a low-dimensional *contact space.* First, contact space can be used to compute the layout of all possible basket grasps of an object waiting to be lifted at a given position. Second, the *depth* (and hence security) of a candidate basket grasp can be computed along the basket-grasp contour in contact space. The main result of the paper, the *basket grasp theorem,* states that the depth of a basket grasp is determined by the relative height of the object's center of mass at specific single and two-finger equilibrium stances associated with the basket grasp. These stances can be readily found and sorted in contact space as demonstrated with detailed examples. Third, the critical *drop-off* event that allows release of the object at its intended destination is associated with a frictionless two-finger equilibrium grasp of the object (without gravity), that can be computed as a simple search in contact space.

In future research, it is natural to seek *quality measures* that will guide the selection of optimal basket grasps. It seems that the basket-grasp depth (which affects quality) *increases* as the fingers open apart. However, the allowed finger opening must satisfy a user-specified margin of security away from the critical drop-off event. Finally, our future work will focus on synthesizing basket grasps using 3-D robot hands. It is a natural extension of this paper, with possible follow-up on the role of the *hand's palm* in performing safe transition from basket grasps to fully secure *immobilizing grasps* of 3-D objects.

Acknowledgement: This work was partially supported by grant no. 1253/14 of the Israel Science Foundation.

REFERENCES

[1] T. F. Allen. *Two and Three Finger Caging of Polygons and Polyhedra*. PhD thesis, Dept. of Mechanical Engineering, Caltech, 2016.

[2] T. F. Allen, E. Rimon, and J. W. Burdick. Two-finger caging of polygonal objects using contact space search. *IEEE Trans. on Robotics*, 31(5), 1164-1179, 2015.

[3] H. A. Bunis and E. D. Rimon. Toward grasping against the environment: Locking polygonal objects against a wall using two-finger robot hands. *IEEE Robotics and Automation Letters*, 2018.

[4] H. A. Bunis, E. D. Rimon, T. F. Allen, and J. W. Burdick. Equilateral three-finger caging of polygonal objects using contact space search. *IEEE Trans. Autom. Sci. Eng.*, 15(3):919–931, 2018.

[5] R. Diankov, S. S. Srinivasa, D. Ferguson, and J. Kuffner. Manipulation planning with caging grasps. In *IEEE Int. Conference on Humanoid Robots*, pages 285–292, 2008.

[6] M. Dogar and S. S. Srinivasa. A framework for push-grasping in clutter. In *Robotics: Science and Systems VII*, page Vol. 1, 2011.

[7] M. Goresky and R. MacPherson. *Stratified Morse Theory*. Springer Verlag, New York, 1980.

[8] Z. Hu, W. Wan, and K. Harada. Dual-arm assembly planning considering gravitational constraints. In *Int. Conf. on Intelligent Robots and Systems*, 2019.

[9] D. Kim, Y. Maeda, and S. Komiyama. Caging-based grasping of deformable objects for geometry-based robotic manipulation. *ROBOMECH Journal,*, 6(3), 2019.

[10] T. Kwok, W. Wan, J., C.C.L. Wang, J. Yuan, K. Harada, and Y. Chen. Rope caging and grasping. In *IEEE Int. Conf. on Robotics and Automation*, pages 1980–1986, 2016.

[11] M. Laskey, J. Lee, C. Chuck, D. Gealy, W. Hsieh, F. T. Pokorny, A. D. Dragan, and K. Goldberg. Robot grasping in clutter: Using a hierarchy of supervisors for learning from demonstrations. In *IEEE Int. Conference on Automation Science and Engineering*, pages 827–834, 2016.

[12] R. R. Ma, W. G. Bircher, and A. M. Dollar. Modeling and evaluation of robust whole-hand caging manipulation. *IEEE Trans. on Robotics*, 35(3):549–563, 2019.

[13] J. Mahler, F. T. Pokorny, Z. McCarthy, A. F. van der Stappen, and K. Goldberg. Energy-bounded caging: Formal definition and 2-D energy lower bound algorithm based on weighted alpha shapes. *IEEE Robotics and Automation Letters*, 1(1):508–515, 2016.

[14] S. Makita and W. Wan. A survey of robotic caging and its applications. *Advanced Robotics*, 31(19-20): 1071–1085, 2017.

[15] P. Pipattanasomporn, T. Makapunyo, and A. Sudsang. Multifinger caging using dispersion constraints. *IEEE Trans. on Robotics*, 32(4), 1033-1041, 2016.

[16] P. Pipattanasomporn, P. Vongmasa, and A. Sudsang. Caging rigid polytopes via finger dispersion control. *IEEE Int. Conf. on Robotics and Automation*, pages 1181–1186, 2008.

[17] E. Rimon and A. Blake. Caging planar bodies by 1-parameter two-fingered gripping systems. *Int. J. of Robotics Research*, 18(3):299–318, 1999.

[18] E. D. Rimon and J. W. Burdick. *The Mechanics of Robot Grasping*. Cambridge University Press, 2019.

[19] E. D. Rimon, F. T. Pokorny, and W. Wan. Configuration space characterization of two-finger basket grasps of 2-D objects. Tech. report, Mechanical Engineering, Technion, https://robots.net.technion.ac.il/publications, Jan. 2020.

[20] A. Rodriguez, M. T. Mason, and S. Ferry. From caging to grasping. *Int. J. Rob. Res.*, 31(7), 886-900, 2012.

[21] J. Su, H. Qiao, Z. Ou, and Z. Liu. Vision-based caging grasps of polyhedron-like workpieces with a binary industrial gripper. *IEEE Trans. on Automation Science and Engineering*, 12(3):1033–1046, 2015.

[22] M. Vahedi and A. F. van der Stappen. Caging polygons with two and three fingers. *Int. J. Robotics Research*, 27(11-12):1308–1324, 2008.

[23] W. Wan and R. Fukui. Efficient planar caging test using space mapping. *IEEE Trans. Autom. Sci. Eng.*, 15(1):278–289, 2018.